



## ON THE ANOMALOUS TEMPERATURE DEPENDENCE OF FATIGUE-CRACK GROWTH IN $\gamma$ -BASED TITANIUM ALUMINIDES

A.L. McKelvey, K.T. Venkateswara Rao\* and R.O. Ritchie  
Department of Materials Science and Mineral Engineering  
University of California, Berkeley, CA 94720-1760

(Received May 30, 1997)

(Accepted August 12, 1997)

### Introduction

Recently, there has been considerable interest in  $\gamma$ -TiAl based titanium aluminides as light-weight structural materials, particularly in the aerospace industry where they are under consideration for gas-turbine engine applications. As they are candidate materials for elevated temperature use, an understanding of their fatigue and fracture properties at temperatures comparable to operating conditions is essential. In this regard, an anomalous temperature dependence of fatigue-crack propagation and the fatigue threshold ( $\Delta K_{TH}$ ) has been reported for  $\gamma$ -based alloys between 25° and 800-850°C in the air environments (1-5). Specifically, near-threshold growth rates are lower at 800°C and higher at 600°C compared to room temperature; similarly, thresholds are highest at 800°C and lowest at 600°C, with 25°C behavior in between. Based on observations that the effect is less striking *in vacuo* compared to air, Larsen *et al.* (5) attributed such behavior to environmental embrittlement and a lack of ductility at intermediate temperatures (on the assumption that  $\Delta K_{TH}$  should increase with increasing temperature in the absence of embrittlement). Since this latter assumption is questionable, we consider here the role of crack-surface oxidation and its tendency to retard crack-growth rates, particularly at near-threshold levels, via crack-tip blunting and shielding by oxide-induced crack closure. In this study, the role of this mechanism on fatigue-crack growth rates in  $\gamma$ -based titanium aluminides is evaluated as a function of temperature, and an alternative explanation is presented for the anomalous temperature dependence of the near-threshold fatigue behavior.

### Experimental Methods

The intermetallic material studied was an XD<sup>TM</sup> processed Ti-47.4Al-1.9Nb-0.9Mn (at.%) alloy containing ~1 vol.% TiB<sub>2</sub> particles (6). Following casting and hot-isostatic pressing at 1260°C and 172

---

\*Currently at Advanced Cardiovascular Systems, Guidant Corporation, 3200 Lakeside Drive, Santa Clara, CA, 95052-8167.

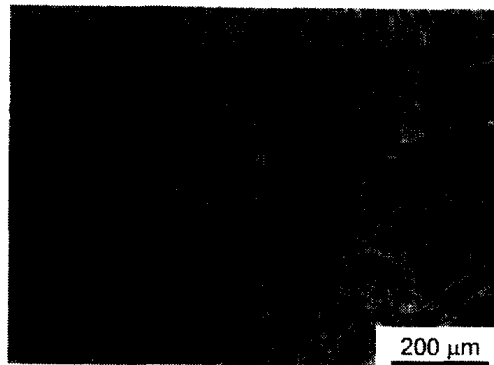


Figure 1. Optical micrograph of the XD<sup>TM</sup>-processed Ti-47.4Al-1.9Nb-0.9Mn (at.%) alloy containing ~1 vol.% TiB<sub>2</sub> particles, heat treated to a fine lamellar ( $\gamma + \alpha_2$ ) microstructure with ~30 vol.% equiaxed  $\gamma$  grains along lamellar colony boundaries (etchant: 2% HF, 5% H<sub>3</sub>PO<sub>4</sub>).

MPa (4 hr), the microstructure consisted of fine lamellar ( $\gamma + \alpha_2$ ) colonies, ~120  $\mu\text{m}$  in size, with ~30 vol.% of equiaxed  $\gamma$  grains, of average diameter ~23  $\mu\text{m}$ , present along lamellar colony boundaries (Fig. 1). The TiB<sub>2</sub> phase was present as blocky particles, (1-5  $\mu\text{m}$  in size), and needle shaped particles, (~20-50  $\mu\text{m}$  long, 3-5  $\mu\text{m}$  in diameter).

Fatigue-crack propagation tests were conducted using disk-shaped compact-tension DC(T) specimens (27 mm wide by 5 mm thick), which were cycled in air at 600° and 800°C, i.e., below and above the ductile-to-brittle transition temperature (DBTT) for  $\gamma$ -TiAl, ~700°C (7). Fatigue tests were performed at 10 Hz (sine wave) under automated stress-intensity ( $K$ ) control, in general accordance with the procedures described in ASTM Standard E647. Crack-propagation rates were measured as a function of the applied stress intensities,  $\Delta K = K_{\text{max}} - K_{\text{min}}$ , at constant positive load ratios of  $R = 0.1$  and 0.5, defined as the ratio of the minimum to maximum stress intensities in the loading cycle ( $R = K_{\text{min}}/K_{\text{max}}$ ). Load shedding at a  $K$ -gradient of -0.1 through -0.07  $\text{mm}^{-1}$  was used to approach the fatigue threshold,  $\Delta K_{\text{TH}}$ , which was defined where growth rates did not exceed ~10<sup>-10</sup> m/cycle. Crack lengths were continuously monitored using load-line based compliance methods and via optical observation through a sapphire port in the furnace using a high-resolution telescope. Good agreement, to within  $\pm 200 \mu\text{m}$ , was obtained between compliance and telescopic measurements. Corresponding results at 25°C for the same alloy are included for comparison (8).

An attempt was made to directly measure the extent of crack closure by estimating the closure stress intensity,  $K_{\text{cl}}$ , corresponding to the load where first deviation from linearity occurred with respect to displacement on unloading. Where closure occurs, an effective (near-tip) stress-intensity range,  $\Delta K_{\text{eff}} = K_{\text{max}} - K_{\text{cl}}$ , can be defined when  $K_{\text{cl}} \geq K_{\text{min}}$  (9). However, as the remoteness of measurement at elevated temperatures made precise definition difficult, estimates for  $K_{\text{cl}}$  were instead calculated from oxide thickness measurements. Auger spectroscopy in combination with focused-ion beam sputtering were used to measure the total oxide thickness on the fracture surfaces after final fracture. The sputtering rate for this alloy was calibrated by using a profilometer and a 1000 Å thick tantalum-oxide film in conjunction with the spectroscopy. X-ray diffractometry, at grazing incident angles of 1°, 5° and 35°, was used to determine the constituents of the oxide films. At 800°C where the oxide scales were approaching micrometer dimensions, measurements were made on nickel-plated metallographic sections, machined perpendicular to the fracture surfaces of fatigue surfaces of fatigue cracks arrested at  $\Delta K_{\text{TH}}$ .

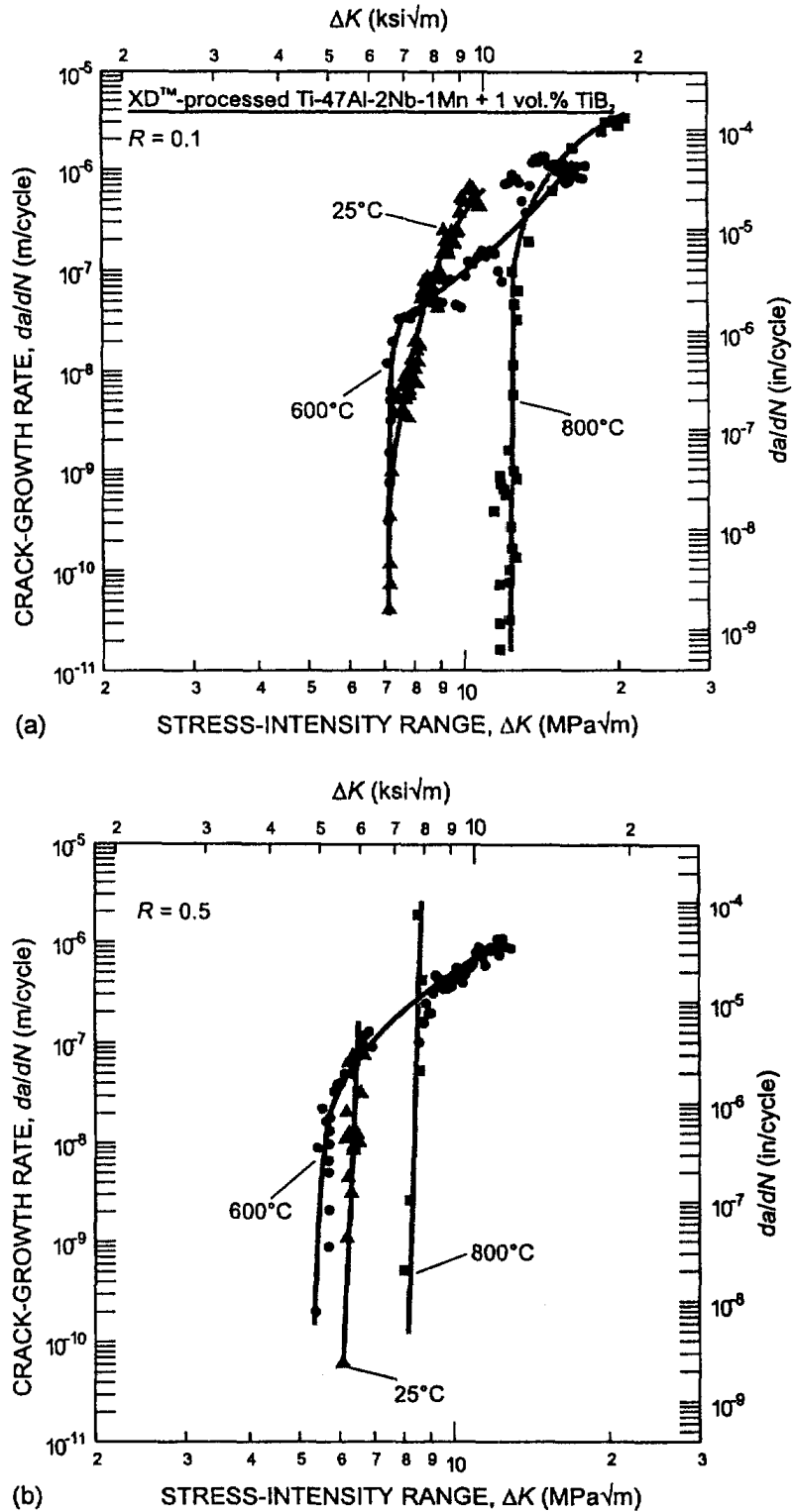


Figure 2. Variation of fatigue-crack propagation rates,  $da/dN$ , with temperature (25°, 600° and 800°C) at (a)  $R = 0.1$  and (b)  $R = 0.5$  in the XD<sup>TM</sup>-processed Ti-47.4Al-1.9Nb-0.9Mn (at.%) alloy containing ~1 vol.% TiB<sub>2</sub> particles. Note how the fatigue thresholds are lowest at 600°C and highest at 800°C, with 25°C data in between.

### Results and Discussion

Rates of fatigue-crack propagation at 25°, 600° and 800° C in air are shown in Fig. 2 for load ratios of 0.1 and 0.5. It is apparent that the fastest near-threshold growth rates ( $<10^{-7}$  m/cycle) and lowest  $\Delta K_{TH}$  values were measured at 600°C, just below the DBTT for TiAl, whereas the slowest near-threshold growth rates and highest thresholds were observed above the DBTT at 800°C; behavior at 25°C was intermediate. As noted above, this anomalous variation in fatigue-crack growth rates with temperature is a characteristic of many  $\gamma$ -TiAl alloys (1-5). It is known that this phenomenon is effectively suppressed for crack growth *in vacuo* (5); the present study further indicates that it is more pronounced at  $R = 0.5$  compared to 0.1 and is absent at higher growth rates above  $\sim 5 \times 10^{-8}$  m/cycle (Fig. 2).

An explanation for this effect proposed by Larsen *et al.* (1,2,5) is that since  $\Delta K_{TH}$  thresholds would normally increase with increasing temperature (in the absence of environmental effects), the data at 600-650°C are "anomalous" due to some unspecified environmental embrittlement at this temperature. In addition, it has been suggested that the effect is related to the increase in ductility above the DBTT at 800°C (3,4). However, most models for intrinsic fatigue-crack growth imply that growth rates should increase, and  $\Delta K_{TH}$  should *decrease*, with increasing temperature (e.g., the simple crack-tip opening displacement model (10) where growth rates are inversely proportional to the yield strength and modulus). Accordingly, a much more probable explanation is that the 800°C data are "anomalous", particularly since the experimental data (5) *in vacuo* show that thresholds decrease with temperature.

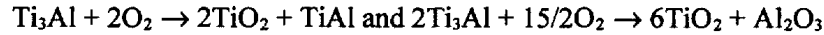
To explain any anomaly in the 800°C data, we note that the effect is most prevalent at near-threshold levels, which suggests a prominent role of crack closure; moreover, since high-temperature air environments are involved, a likely candidate is closure induced by oxidation products (11). To evaluate the influence of oxide-induced crack closure (OICC) at the temperatures in question, Auger spectroscopy was used in combination with sputtering techniques and metallography to measure the peak thickness of the oxide deposits on the fatigue fracture surfaces as a function of temperature and load ratio (Table 1).

Since OICC, in the form of premature contact of the crack surfaces on unloading, may be considered to be active when the peak oxide thickness is comparable with the minimum crack-tip opening displacement ( $CTOD_{min}$ ) in the loading cycle, these data strongly suggest that closure is significantly more active at 800°C than at 25°C and 600°C. However, it is the *excess* oxide volume inside the crack allowing for the conversion of metal that is important in this comparison (12). To compute these values, it is necessary to know the prevailing oxidation reaction(s). Using X-ray diffractometry to identify the oxide constituents, it was found that  $TiO_2$  and  $Al_2O_3$  exhibited the strongest characteristic peaks at both 600° and 800° C, indicating that  $TiO_2$  and  $Al_2O_3$  occupy the largest mole fraction of the oxide layer; smaller amounts of TiN,  $Ti_3AlN$ , pure Ti and  $MnO_2$  were also detected. To determine the thickness of excess material on the fracture surfaces, the volume ratio of oxide to metal of an oxidation reaction,

TABLE I  
Total Thickness of Oxide on Fatigue Surfaces, Estimated  $CTOD_{min}$ , and Excess Oxide Thickness at  
25°-800°C in Air at  $\Delta K_{TH}$

	25°C			600°C			800°C		
	thickness, nm	$CTOD_{min}$ nm	excess thickness, d nm	thickness, nm	$CTOD_{min}$ nm	excess thickness, d nm	thickness, nm	$CTOD_{min}$ nm	excess thickness, d nm
$R = 0.1$	17 ± 10	2.5	13	230 ± 12	4	175	726 ± 81	11	552
$R = 0.5$	22 ± 8	154	17	120 ± 10	170	91	266 ± 11	430	202

*i.e.*, the Pilling-Bedworth (P-B) ratio (13), was determined. To simplify the analysis, reactions which only consider the formation of  $\text{TiO}_2$  and  $\text{Al}_2\text{O}_3$ , were used to approximate the actual P-B ratio:



These reactions represent upper and lower bounds for the P-B ratios, which have values of 1.56 and 1.14 respectively. Since the oxide layer may have resulted from several reactions simultaneously, the bulk P-B ratio was taken as the average value of 1.32 in order to calculate excess oxide thicknesses. These thicknesses are compared with corresponding  $CTOD_{\min}$  values at  $\Delta K_{\text{TH}}$  in Table 1 to give a clear indication of the relative effects of OICC over the temperature range in question.

Further insight can be gained by estimating the closure stress intensities,  $K_{\text{cl}}$ , by assuming that the oxide is a rigid wedge inside the crack (12), viz:

$$K_{\text{cl}} = \frac{Ed}{4\sqrt{\pi l}(1-\nu^2)} \quad (1)$$

where  $d$  is the peak excess oxide thickness,  $2l$  is its location behind the tip,  $E/(1-\nu^2)$  is the effective Young's modulus in plane strain, and  $\nu$  is Poisson's ratio. From Eq. 1, values of  $K_{\text{cl}}$  at  $25^\circ$  and  $600^\circ\text{C}$  were estimated, respectively, to be 0.3 and 3.1  $\text{Mpa}\sqrt{\text{m}}$  at a load ratio of 0.1 and  $\sim 0.3$  and 1.6  $\text{Mpa}\sqrt{\text{m}}$  at  $R = 0.5$ . At  $800^\circ\text{C}$ ,  $K_{\text{cl}}$  values were considerably greater with corresponding estimates being, respectively, 9.8 and 3.6  $\text{Mpa}\sqrt{\text{m}}$  at load ratios of 0.1 and 0.5.

From these considerations, it is apparent that the role of OICC at  $25^\circ\text{C}$  is small (e.g.,  $K_{\text{cl}} < K_{\min}$  at low  $R$ ); indeed it is essentially negligible at  $R = 0.5$  where  $d \ll CTOD_{\min}$ . At  $600^\circ\text{C}$ , the role of OICC is still relatively minor, as  $d < CTOD_{\min}$  at  $R = 0.5$ ; even at  $R = 0.1$ ,  $K_{\text{cl}}$  values are still only a small fraction of  $K_{\max, \text{TH}}$ , *i.e.*,  $K_{\text{cl}}/K_{\max, \text{TH}} < 0.39$ . However, at  $800^\circ\text{C}$ , the extent of crack-surface oxidation is extensive,  $d \gg CTOD_{\min}$  at  $R = 0.1$ , such that the reduction in the near-tip driving force for crack extension due to oxide wedging is substantial (*i.e.*,  $K_{\text{cl}}/K_{\max} \sim 0.77$  at  $\Delta K_{\text{TH}}$ ).

Since fatigue-crack propagation can be considered as the mutual competition of intrinsic microstructural damage mechanisms ahead of the crack tip, which *promote* crack advance, and extrinsic crack-tip shielding (e.g., closure) mechanisms, behind the tip, which act to *impede* it (15), we conclude that the anomalous temperature effect on the near-threshold fatigue of  $\gamma$ -TiAl based alloys results directly from this interplay. Indeed, if the crack-growth rates in Fig. 2 are replotted as a function of  $\Delta K_{\text{eff}}$  after "correcting" for such closure (Fig. 3), the anomalous temperature dependence disappears. Rather than growth rates being accelerated (and  $\Delta K_{\text{TH}}$  thresholds lowered) at intermediate temperatures due to some unspecified environmental embrittlement (1,2,5) and a lack of ductility below the DBTT (3,4), it is proposed that as the intrinsic fatigue resistance decreases with increasing temperature (as seen *in vacuo* (5)), growth rates are instead retarded (and  $\Delta K_{\text{TH}}$  increased) at  $800^\circ\text{C}$  due to the substantial effect of crack closure from the wedging of crack-surface oxidation products. This explanation is consistent with the *in vacuo* results (5), all oxidation data (Table 1), and simple intrinsic models for fatigue-crack growth (10). Moreover, the sudden onset of threshold behavior at high growth rates, shown by the  $800^\circ\text{C}$  data (Fig. 2), is very characteristic of the cessation of crack growth due to thermal oxide wedging (e.g., (16)).

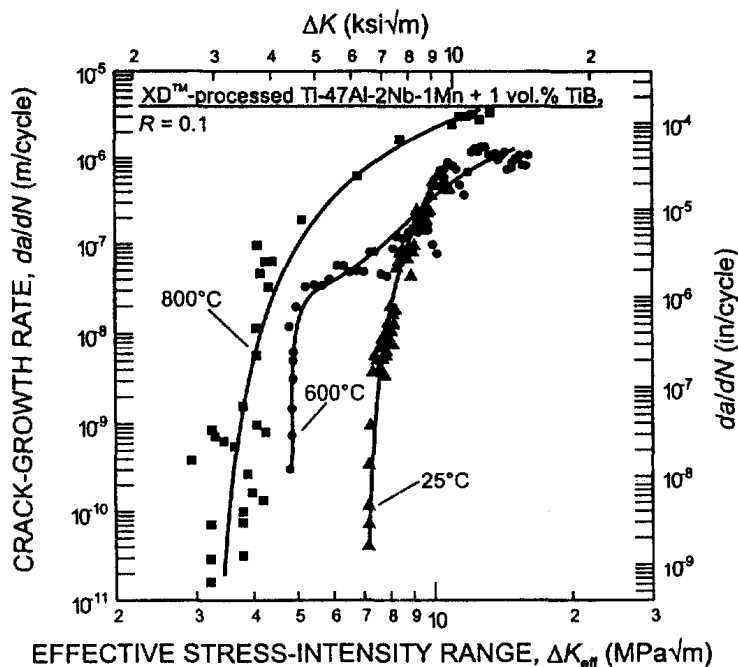


Figure 3. Variation of fatigue-crack propagation rates,  $da/dN$ , at  $R = 0.1$  with the effective stress-intensity range ( $\Delta K_{\text{eff}} = K_{\text{max}} - K_{\text{cl}}$ ) in the XD<sup>TM</sup>-processed Ti-47.4Al-1.9Nb-0.9Mn (at.%) alloy containing  $\sim 1$  vol.% TiB<sub>2</sub> particles. Note how after "correcting" for crack closure, the "anomalous temperature effect" on fatigue thresholds disappears.

### Conclusions

Based on a study on the fatigue-crack growth behavior at  $R = 0.1$  and  $0.5$  between  $25^\circ$  and  $800^\circ\text{C}$  in a  $\gamma$ -TiAl based XD<sup>TM</sup> Ti-47.4Al-1.9Nb-0.9Mn (at.%) alloy (with  $\sim 1$  vol.% TiB<sub>2</sub> particles), with a fine lamellar microstructure, the following conclusions can be made:

1. An anomalous temperature effect on fatigue-crack propagation rates is confirmed in that growth rates are found to be lower at  $800^\circ\text{C}$ , yet higher at  $600^\circ\text{C}$ , than at  $25^\circ\text{C}$ ; similarly  $\Delta K_{\text{TH}}$  thresholds are highest at  $800^\circ\text{C}$  and lowest at  $600^\circ\text{C}$ , with room temperature behavior in between. The effect, however, is only seen in air environments and predominates at near-threshold levels below  $\sim 5 \times 10^{-8}$  m/cycle.
2. Rather than being associated with some unspecified embrittlement at  $600^\circ\text{C}$ , the effect is ascribed to a dominant role of oxide-induced crack closure at  $800^\circ\text{C}$ , which retards near-threshold crack growth rates and results in a premature arrest of crack growth at a higher  $\Delta K_{\text{TH}}$  threshold value. This explanation is consistent with results *in vacuo*, Auger spectroscopy measurements of crack-surface oxidation debris, and simple intrinsic models for fatigue-crack growth.

### Acknowledgments

This work was funded by the Air Force Office of Scientific Research under Grant No. F49620-96-1-0233. Thanks are due to Dr. C.B. Ward for his support, to Dr. P. Hou, Dr. W. MoberlyChan and J.P.

Campbell for helpful discussions, the National Science Foundation for a graduate fellowship for ALM, and General Motors Corp. for supplying the alloy.

### References

1. S.J. Balsone, J.W. Jones and D.C. Maxwell, in *Fatigue and Fracture of Ordered Intermetallic Materials: I*, eds. W.O. Soboyejo, T.S. Srivatsan and D.L. Davidson, p. 307 TMS (1994).
2. S.J. Balsone, J.M. Larsen, D.C. Maxwell and J.W. Jones, *Mater. Sci. Eng. A* **192/193**, 457 (1995).
3. J.M. Larsen, B.D. Worth, S.J. Balsone and J.W. Jones, in *Gamma Titanium Aluminides*, eds. Y.-W. Kim, R. Wagner and M. Yamaguchi, p. 821, TMS, Warrendale, PA (1995).
4. K.T. Venkateswara Rao, Y.-W. Kim and R.O. Ritchie, *Scripta Metall. Mater.* **33**, 459 (1995).
5. J.M. Larsen, B.D. Worth, S.J. Balsone, A.H. Rosenberger and J.W. Jones, in *Fatigue '96*, eds. G. Lütjering and H. Nowack, 6th Intl. Conf. on Fatigue, p. 1719, Pergamon, Oxford, (1996).
6. D.E. Larsen and M. Behrendt, in *Fatigue and Fracture of Ordered Intermetallic Materials: I*, eds. W.O. Soboyejo, T.S. Srivatsan and D.L. Davidson, p. 27, TMS, Warrendale, PA (1994).
7. H.A. Lipsitt, D. Schectman and R.E. Schafrik, *Metall. Trans. A* **6**, 1991 (1975).
8. J.P. Campbell, K.T. Venkateswara Rao and R.O. Ritchie, in *Fatigue '96*, eds. G. Lütjering and H. Nowack, 6th Intl. Conf. on Fatigue, p. 1779, Pergamon, Oxford (1996).
9. W. Elber, *Eng. Fract. Mech.* **2**, 37 (1970).
10. F.A. McClintock, in *Fatigue Crack Propagation*, ASTM STP 415, p. 170, American Society Testing Materials, Philadelphia, (1967).
11. S. Suresh, G.F. Zamiski and R.O. Ritchie, *Metall. Trans. A* **12**, 1435 (1981).
12. S. Suresh and R.O. Ritchie, *Eng. Fract. Mech.* **18**, 785 (1983).
13. O. Kubaschewski and B.E. Hopkins, *Oxidation of Metals and Alloys*, Academic Press, New York (1953).
14. S. Suresh and R.O. Ritchie, in *Fatigue Crack Growth Threshold Concepts*, eds. D.L. Davidson and S. Suresh, p. 227, TMS, (1984).
15. R.O. Ritchie, *Mater. Sci. Eng. A* **103**, 15 (1988).
16. J.L. Yuen, P. Roy and W.D. Nix, *Metall. Trans. A* **15**, 1769 (1984).